Effects of aggregation on the blood flow velocity field measured by a μPIV based technique

Efstathios KALIVIOTIS*, Jonathan DUSTING, Stavroula BALABANI

*Corresponding author: Tel.: ++44 (0)207 8482041; Fax: ++44 (0)207 8482902;
Email: efstathios.kaliviotis@kcl.ac.uk
ECLAT, Division of Engineering, King's College London, UK

Abstract The flow of red blood cells is investigated by means of a micro-PIV based technique at physiological hematocrit levels and in the presence of aggregation. The technique developed differs from typical micro-PIV as the RBCs are used as tracer particles and illumination is provided by a simple halogen light source. Changes in the microstructure of blood caused by aggregation were observed to affect the RBC flow characteristics in a narrow-gap plate-plate geometry. At low shear rates, high aggregation caused the RBC motion to become essentially two-dimensional and network formation lead to the flow deviating from the expected radial profile. The accuracy of the micro-PIV technique was shown to be dependent on aggregation, illustrating the need to take aggregation into account in future RBC flow studies.

Keywords: Micro-scale blood flow, RBC network formation, aggregates

1. Introduction

Understanding the behaviour of blood flow in the circulatory system is important to many physiological and pathological conditions. Blood is a complex, non-Newtonian, multiphase system; its haemodynamics and rheology depend on many factors such as the volume fraction (hematocrit) and the aggregation tendency of the red blood cells (RBCs). While *in vivo* blood flow measurements are important for detecting the onset or causes of many vascular diseases, at present the blood flow velocity field cannot easily be resolved with sufficient spatial or temporal resolution. *In vitro* measurements are still required to provide insight into many haemodynamic phenomena.

The aggregation phenomenon which occurs between the RBCs has a significant effect on the mechanical properties of blood; viscoelastic behaviour and increased viscosity is observed at low compared to high shear rates and even a yield stress exists at very low shear rates (Baskurt and Meiselman 2003). The increase in viscosity of blood is due to the microstructural changes that take place in the fluid at the specific flow conditions; aggregative forces acting on the biconcave shaped RBCs have as a result the formation of rouleaux (structures resembling coin piles), the formation of spherical aggregates from the aggregation of rouleaux and the formation of an extended RBC network from interconnected rouleaux and aggregates. The plasma macromolecular composition (mainly fibrinogen) and the intrinsic aggregative properties of the RBCs determine the development and intensity of the aggregative forces although the exact mechanism of the intercellular attraction is still not clear (Rampling 1989). Fluid shearing forces acting on the aggregates are responsible for their break-down.

RBC aggregation has been extensively investigated in the past five decades through the use of various techniques and valuable information has been obtained regarding its effects on blood rheological behaviour. Aggregation measurement techniques could be categorised as indirect and direct. Indirect techniques include for example techniques based on the measurement of the light transmitted or back-scattered by the blood

sample. Direct techniques involve the measurement of aggregate characteristics via direct observation with the aid of light microscopy (see Rampling and Whittingstall (1986) for a study on the comparison between techniques). Direct data quantifying the effect of the microstructural changes of blood, occurring due to RBC aggregation, on the velocity field have not been reported in the literature.

Micro-PIV is a powerful measurement technique that has been applied to a variety of biological and non-biological micro flow problems over the past decade. It typically involves the imaging of fluorescent particles illuminated with a laser, and then cross-correlation of image pairs of known time separation to provide velocity estimates. Division of the images into small interrogation windows enables spatial resolution of the velocity field in two dimensions, while the use of multiple cameras and/or more sophisticated processing techniques can facilitate three-dimensional or three-component measurement. Micro-PIV techniques have been employed in recent years to characterize the blood flow field both *in vivo* and *in vitro*; for example Hove et al. (2003) studied the shear stresses developed in the cardiac chamber of a fish embryo, Lee, Ji and Lee (2007) investigated the blood flow in a chicken embryo vessel and Lima et al. (2007) studied the flow of non-aggregated human blood in a microfluidic channel. Due to optical limitations, the hematocrit levels were kept low in the previous *in vitro* studies and the effects of aggregation on the velocity field were not taken into account.

Accurate micro-PIV measurement requires tracers to be distributed throughout the fluid. These tracers must also reliably follow the flow and provide a suitable intensity distribution, within each interrogation window, for good cross-correlation. As we demonstrate in the current paper, it is possible to use the erythrocytes themselves as tracer particles when measuring blood flow velocity fields. This removes the need for fluorescent particles, laser illumination, and an optical filter system.

Human blood samples at normal haematocrit levels (i.e. 45%) were subjected to simple shear flow in a plate-plate geometry and information about the velocity field and aggregation extent was obtained by using image analysis techniques (Dusting et al. 2009). The combined velocity field and aggregation measurements were used to investigate the effect of the microstructural changes on the flow mechanics of blood. Furthermore, the effectiveness of the micro-PIV technique was evaluated for different aggregation characteristics.

2. Methodology

Blood samples (30 ml of blood after a 12-hour overnight fast) were provided by healthy volunteers according to King's College Research Ethics Committee guidelines (CREC ref. 04/05-15). Samples were collected in bottles of 10 ml preloaded with 1.2% anticoagulant agent EDTA (ethylene-diamine-tetraacetic-acid). The hematocrit of the sample was determined by centrifugation (3000 rpm for 10 minutes) and adjusted to 45% (packed cell volume) by subtracting or adding plasma. Testing was completed within approximately four hours of sample collection.

An optical shearing system, as shown in Fig. 1, was used in this study. This consisted of two parallel glass plates set apart by a gap h=30 μm. The bottom plate was rotated while the upper plate was held stationary. Different nominal shear rates $\dot{\gamma}$ (5.4, 11.7, 25.2, 54, 117 and 252 s^{-1}) were set by adjusting the angular velocity of the bottom plate (ω); the nominal shear rate $\dot{\gamma}$ was expected to vary slightly over the observation region. The radial position (R) of the centre of the observation area was 7.5 mm. With such a small gap distance the distribution of RBCs was similar to, but not exactly, a two-dimensional layer. The small gap used in the study (30 μm) differs from that utilised in concentric cylinder

geometries (approximately 1 mm) for the measurements of aggregation; this characteristic, however, was important for the measurement of velocity and aggregation, as both techniques use 2D images of a 3D illuminated field, and any deviation from 2D behaviour is not resolved. For standard micro-PIV, gradients in the *z* direction reduce the measurement accuracy as tracers at different depths contribute unequally to the overall cross-correlation peak (Olsen and Adrian 1999). The small gap, coupled with a numerical aperture of 0.25, meant that a relatively large portion of the gap lay within the depth of focus. In addition, taking into account the likely migration of cells away from the walls it can be assumed that the majority, if not all, of the cells were captured in the images.

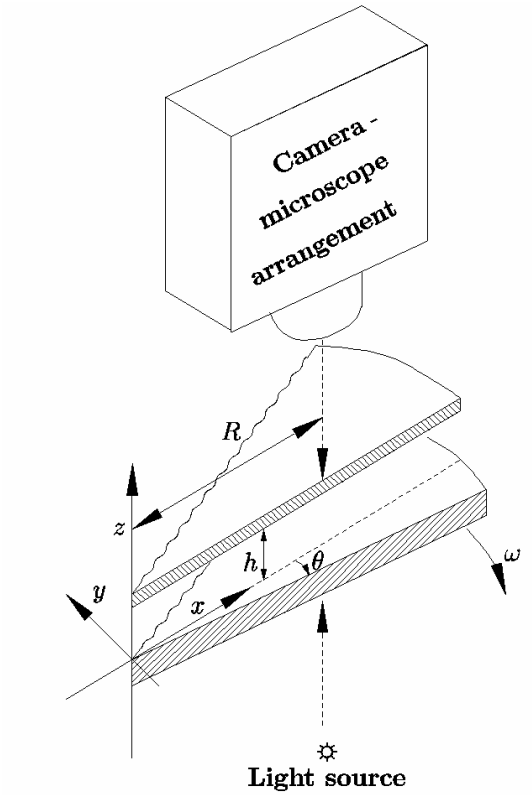

Fig. 1 Schematic representation of the plate-plate system used in the study

The plate-plate test section was mounted in the microscope and illuminated by a halogen lamp. A high speed CMOS camera with a 1280 x 1024 pixel resolution was employed to obtain images of the sheared blood flow field at a 10 times magnification. The images were cross correlated using commercial PIV software (Flow Manager, Dantec Dynamics). An adaptive cross correlation technique was employed with a final interrogation area of 64x64 pixels and 50% overlapping. The captured images were further processed to determine the degree of aggregation by using a previously developed aggregation index A_a (Kaliviotis and Yianneskis 2008); $A_\alpha = S_f / (1-H)S_o$, where S_f is the apparent cell free area, H is the hematocrit and S_o is the total area of observation.

The measurement system differed from traditional micro-PIV systems, as artificial tracer particles, a laser, and optical filters were not required. The ability to obtain suitable intensity fields for cross-correlation, i.e. the ability to use blood cells as tracer particles, resulted from three important factors associated with the experimental set-up. Firstly, the relatively small size of the gap meant that the number of imaged cells/aggregates provided a suitable 'particle' density for micro-PIV. As discussed in further detail later in the paper, this tracer density varies as a function of cell aggregate size so the accuracy of the technique was found to vary with the extent of aggregation. Secondly, back-illumination of the erythrocytes provided adequate particle image contrast. Thirdly, a camera with a suitably high frame-rate (up to 175 frames per second) was used so that the particle displacement between images was appropriate.

3. Coupled velocity and aggregation

Fig. 2 below shows two typical images of blood under flow obtained at shear rates of 117 and 25.2 s^{-1}. Upon careful inspection, distinct red blood cell aggregates and white areas (the plasma gaps) can be observed in the 25.2 s^{-1} case, whereas at 117 s^{-1} the RBCs appear more separated, resulting in a more uniform intensity distribution across each image.

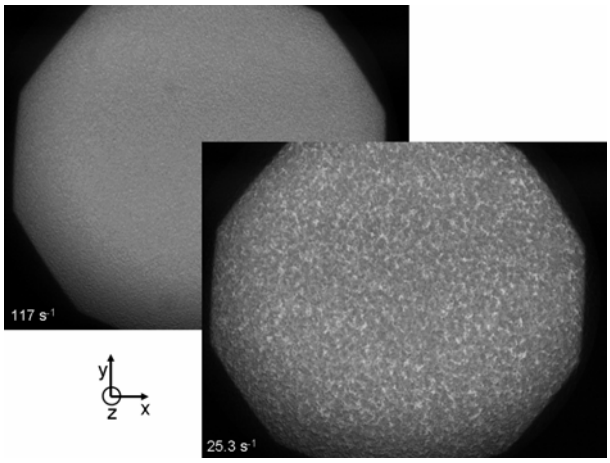

Fig. 2 Representative images captured at shear rates of 117 and 25.2 s^{-1}.

Time-averaged velocity fields captured at different microscope objective positions for a shear rate of 54 s^{-1} are shown in Fig. 3. The four different fields represent different microscope lens objective positions, where z_f represents the centre of focus in the vertical direction, i.e. the direction perpendicular to the plates, and where z_f=0 was determined by focusing on the bottom plate. It should be noted that due to the volume-illuminated nature of the technique the multiple velocity fields shown in Fig. 3 do not represent a reconstruction of the flow in 3D space. While the velocity magnitudes |v| are mostly uniform, it is apparent that at this shear rate there is a slight increase, as highlighted by coloured contours, of |v| as a function of rotating plate radius and focal position. Aggregates are known to be dispersed above 50 s^{-1} in samples with normal aggregation characteristics (Schmid-Schoenbein et al. 1973). For the dispersed state the flow of RBCs at normal concentrations is complex; cells have been observed to continuously deform and change shape due to cell-cell interactions, suggesting also that their membranes may rotate about their inner centre (Goldsmith and Marlow 1979). Fig. 3 indicates that the cells are sufficiently dispersed to vary in the radial direction and even across the relatively thin gap.

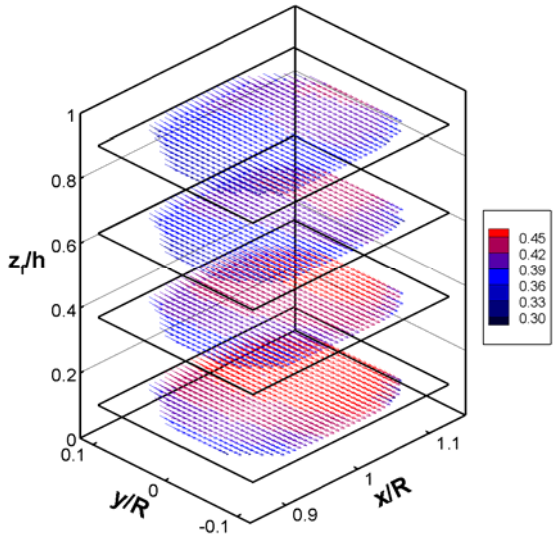

Fig. 3 Time averaged velocity fields for a shear rate of 54.4 s^{-1} and at four different planes of focus. Contours represent the vector magnitude, normalized by ωR.

However, the distinct differences between the velocities at different focal positions (z_f/h) observed in the 54 s^{-1} case were not so apparent at lower shear rates. In Fig. 4 the mean velocity magnitude at a fixed position near the centre of the viewing area is plotted as a function of shear rate ($5.4 \le \dot{\gamma} \le 54$ s^{-1}). Although there is an uncertainty in the measurements taken at the various z_f planes due to the relatively large depth of focus, an expected trend is observed whereby the highest velocity magnitude is measured at the plane closer to the rotating plate (z_f/h = 0.1) and the measured velocities decrease as the centre of focus is moved closer to the stationary plane (i.e as z_f/h increases). Fig. 4 shows that as the shear rate decreases the velocity behaviour deviates from that observed for the 54 s^{-1} case. For instance, the velocities measured at the four different planes of focus for the low shear rates (e.g. 11.7 s^{-1}) are almost identical. This behaviour can be explained by variations in the dominance of the aggregation forces, which result in the formation of rouleaux, larger aggregates and network, with shear rate.

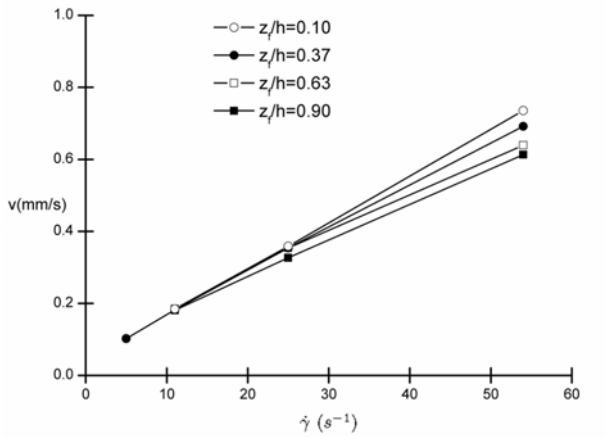

Fig. 4 Mean velocity magnitudes against shear rate at a fixed position near the center of the viewing area for four different positions of focus.

Fig. 5 shows the time averaged aggregation index A_α as a function of shear rate. It is apparent that at 54 s^{-1} the magnitude of the aggregation index is very small, it increases slightly as shear rate is decreased to 25.2 s^{-1}, and increases sharply as the shear rate is decreased to 11.7 and 5.4 s^{-1}. Individual cells have a diameter of approximately one quarter the gap width, and as A_α increases it naturally follows that the aggregates occupy an increasing percentage of the gap width, until eventually they occupy most of the gap.

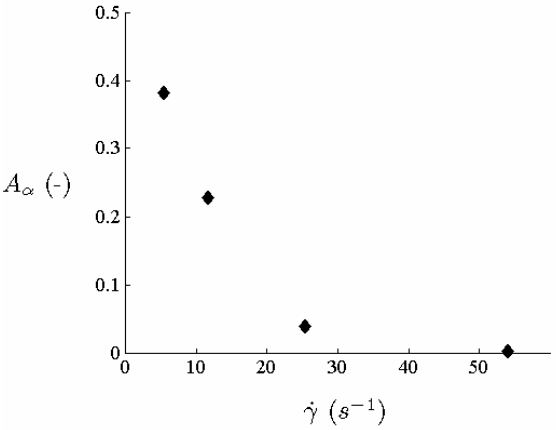

Fig. 5 Time averaged aggregation magnitudes for different shear rates measured at the centre of the images in a window covering the approximately 80% of the viewing area.

As a consequence of this, the measured velocities are more uniform in the *z* direction so that at shear rates at or below 11.7 s^{-1} the cell/aggregate motion is effectively two dimensional. It should be noted however, that only the RBCs have been measured here and therefore from the observations it does not necessarily follows that plasma or other blood components would remain two dimensional. It would be expected that a continuum would have a Couette velocity profile, such that at a radial position R, the tangential velocity, v, is equal to ωR at z=0 and equal to 0 at z=h.

The effect of large aggregation is also apparent in the radial velocity profiles, which are presented in Fig. 6. This figure shows the velocity magnitude, normalised by that at the centre of the viewing field ($|v_o|$), against the expected velocity profile in the normalised radial direction (x/R) for two shear rates, 5.4 and 54 s^{-1} respectively.

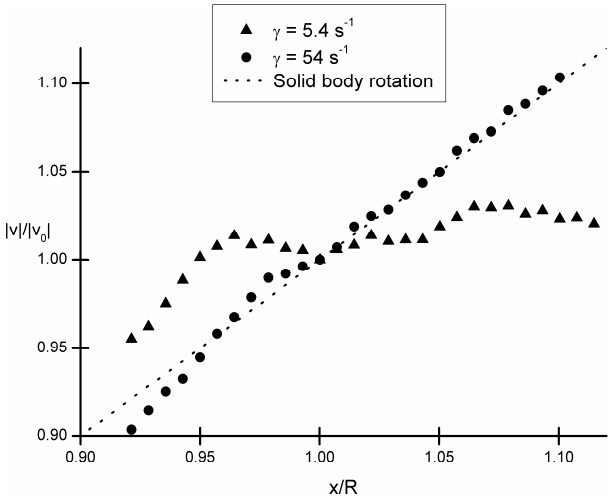

Fig. 6 Velocity magnitudes normalized by the velocity at centre of the viewing field for two different shear rates (5.4 and 54 s^{-1}) against normalised radius (x/R) at y=0. Dotted line represents the expected velocity profile for solid body rotation.

It is clear that the time-averaged velocity profile of the 54 s^{-1} case follows the expected profile for solid body rotation relatively accurately, whereas for the 5.4 s^{-1} case the velocity field deviates sharply from this profile. The change in the velocity profile of the 5.4 s^{-1} case may be attributed to the very

large aggregate size and the resulting formation of a network structure across the x-y plane. The size of the aggregates increases to more than 10 times the RBC diameter, which is equivalent to > 0.01R, and the network formation creates forces between aggregates which strongly influence their relative motion. Changes in the network characteristics, such as the branch size relative to the aggregate size, have been shown to correlate with changes in the mechanical properties of blood (Kaliviotis and Yianneskis 2008).

4. Effect of aggregation on technique accuracy

Aggregation and disaggregation also influence the efficacy of the micro PIV technique used in the present study, which is a simpler alternative to laser-based micro PIV. This is because aggregation characteristics affect the reliability of the flow assumptions and also because aggregation effects the 'particle' image quality.

The first issue, i.e. that the reliability of the flow assumptions is related to aggregation, arises due to the volume illumination. It has been shown in the previous section that as the cells disaggregate and disperse, their motion becomes increasingly three-dimensional, and in particular there is an increased velocity gradient in the *z* direction. The accuracy of the measurements, which are a 2D projection of the velocities in the illuminated volume, may therefore decrease for dispersed cell cases if additional post-processing is not performed.

Furthermore, the technique accuracy is affected by the manner in which the imaged cell 'patterns' change between the fully disaggregated and aggregated states (see Fig. 2 for example). The particle density is known to be a key factor in the accuracy of PIV measurement (Raffel 2007). Similarly, it is necessary to have a suitable ratio between high intensity and low intensity regions of the PIV interrogation windows. When cells are dispersed the intensity distributions within each window may be more uniform, which has a result analogous to reducing the signal to noise ratio. To quantify the effect of these qualitative image changes on the PIV accuracy, the 2D correlation coefficient R_{ij} was calculated for different shear rates as follows:

$$R_{ij} = \frac{\sum_{i=1}^{n}\sum_{j=1}^{n}\left(A_{ij}-\overline{A}\right)\left(B_{ij}-\overline{B}\right)}{\sqrt{\sum_{i=1}^{n}\sum_{j=1}^{n}\left(A_{ij}-\overline{A}\right)^2\sum_{i=1}^{n}\sum_{j=1}^{n}\left(B_{ij}-\overline{B}\right)^2}}$$

Where A_{ij} and B_{ij} were intensities at pixel locations (ij) in two consecutive images, n is the interrogation window size, and $\overline{A}$ and $\overline{B}$ are the window-averaged pixel intensities. Fig. 7 shows the correlation coefficients as a function of radial position for shear rates between 5.4 and 252 s^{-1}. The correlation coefficients are constant across the x domain for each shear rate, however there is a marked difference between each shear rate. For 5.4 and 11.7 s^{-1} the image correlation is very strong, but by 25.2 s^{-1} the R_{ij} value has begun to decrease. By 117 s^{-1} the correlation coefficient is quite low, meaning that it is more difficult to achieve accurate micro-PIV measurements.

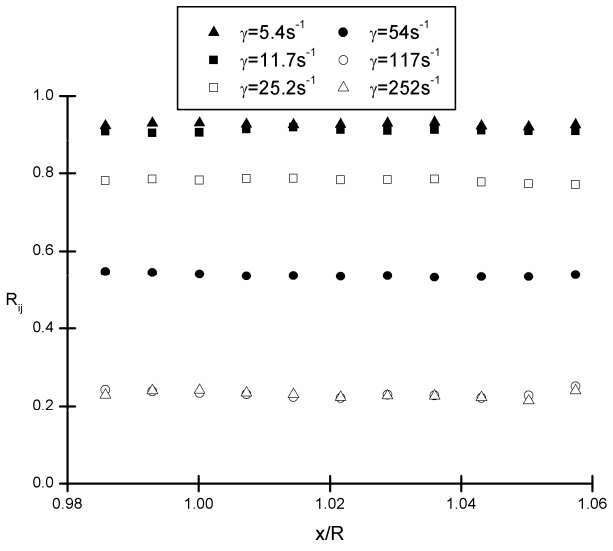

Fig. 7 Image intensity correlation coefficient for four different shear rates across y=0.

It appears from this analysis that aggregation has a positive effect on technique accuracy. Whether this is the case for other experimental

systems may depend on the illumination, objective, and flow apparatus characteristics; however, it is clear that aggregation characteristics should be taken into account when undertaking blood flow measurement using micro PIV.

Another important issue regarding the accuracy of the technique is that measurements reflect the RBC and not the medium fluid velocity characteristics; this fact together with the wall slip phenomenon, caused by the two-phase nature of blood and amplified by the aggregation phenomenon, suggest that deviations from the ideal flow of a continuum fluid would be expected.

5. Conclusions

A simple micro PIV technique was developed in order to measure the velocity of red blood cells in a spatially resolved manner, and therefore study the coupling between blood cell aggregation and velocity. It was found that at the higher shear rates studied the red blood cells were disaggregated and that the velocity measurements depended on the centre of focus. At the lower range of shear rates, where aggregates and network formation were observed, the measured velocities were uniform across the thin gap between the plates, implying that the cell/aggregate motion is essentially two-dimensional. Furthermore, at the lowest shear rate, 5.4 s^{-1}, the flow deviated substantially from the expected solid body rotation profile.

Aggregation was also observed to affect the efficacy of the technique. At high shear rates the dispersed nature of the cells led to the breakdown of the two-dimensionality assumption and lower image quality which may cause reduced correlation. For increased aggregation, correlation was substantially improved. It is therefore recommended that the effects of aggregation should be considered in future blood flow PIV studies.

Acknowledgements

This work was supported in part by the EPSRC Life Sciences Interface program (EP/F007736/1) and by the Leverhulme Trust (F/07 040/X).

References

Baskurt, O. and Meiselman, H.J., 2003. Blood Rheology and Hemodynamics. Seminars in Thrombosis and Hemostasis 29(5), 435-450.

Dusting, J., Kaliviotis, S., Balabani, S., and Yianneskis, M., 2009. Coupled human erythrocyte velocity field and aggregation measurements at physiological haematocrit levels. Journal of Biomechanics 42(10), 1438-1443.

Hove, J., Koster, R., Forouhar, A., Acevedo-Bolton, G., Fraser, S., and Gharib, M., 2003. Intracardiac fluid forces are an essential epigenetic factor for embryonic cardiogenesis. Nature 421, 172–177.

Lee, J., Ji, H., and Lee, S., 2007. Micro-PIV measurements of blood flow in extra embryonic blood vessels of chicken embryos. Physiological Measurement 28, 1149-1162.

Lima, R.,Wada, S., Takeda, M., Tsubota, K., and Yamaguchi, T., 2007. In vitro confocal micro-PIV measurements of blood flow in a square microchannel: The effect of the hematocrit on instantaneous velocity profiles. Journal of Biomechanics 40, 2752–2757.

Lima, R., Ishikawa, T., Imai, Y., Takeda, M., Wada, S., and Yamaguchi, T., 2008. Radial dispersion of red blood cells in blood flowing through glass capillaries: The role of hematocrit and geometry. Journal of Biomechanics 41, 2188–2196.

Kaliviotis, E., and Yianneskis, M., 2008. On the effect of microstructural changes of blood on energy dissipation in Couette flow. Clinical Hemorheology and Microcirculation 39, 235-242.

Olsen, M. and Adrian, R., 2000. Out-of-focus effects on particle image visibility and correlation in microscopy particle image velocimetry. Experiments in Fluids, S166-S174.

Raffel, M., Willert, C. E., Wereley, S. T., and Kompenhans, J., 2007. Particle Image Velocimetry: A Practical Guide. Springer, Berlin, Germany.

Rampling, M., 1989. Red cell aggregation and yield stress. Clinical Blood Rheology 1, 45–63.

Rampling, M. and Whittingstall P., 1986. A Comparison of five Methods for Estimating Red Cell Aggregation. Klinische Wochenschrift 64, 1084–1088.

Schmid-Schoenbein, H., Gosen, J. V., Heinich, L., Klose, H. J. and Volger E., 1973. Counter-rotating rheoscope chamber for study of microrheology of blood-cell aggregation by microscopic observation and microphotometry. Microvascular Research 6 (3), 366–376.